BIOELECTRICITY
Volume 2, Number 1, 2020

DOI: 10.1089/bioe.2019.0032

Original Research

Interferon-Gamma Stimulated Murine Macrophages *In Vitro*: Impact of Ionic Composition and Osmolarity and Therapeutic Implications

Joshua Erndt-Marino, PhD,[1–3] Daniel J. Yeisley, BS,[1] Hongyu Chen, PhD,[1] Michael Levin, PhD,[3] David L. Kaplan, PhD,[2,3] and Mariah S. Hahn, PhD[1]

Abstract

Background: Injections of osmolytes are promising immunomodulatory treatments for medical benefit, although the rationale and underlying mechanisms are often lacking. The goals of the present study were twofold: (1) to clarify the anti-inflammatory role of the potassium ion and (2) to begin to decouple the effects that ionic strength, ionic species, and osmolarity have on macrophage biology.
Materials and Methods: RAW 264.7 murine macrophages were encapsulated in three-dimensional, poly(ethylene glycol) diacrylate hydrogels and activated with interferon-gamma to yield M(IFN). Gene and protein profiles were made of M(IFN) exposed to different hyperosmolar treatments (80 mM potassium gluconate, 80 mM sodium gluconate, and 160 mM sucrose).
Results: Relative to M(IFN), all hyperosmolar treatments suppressed expression of pro-inflammatory markers (nitric oxide synthase-2 [NOS-2], tumor necrosis factor-alpha, monocyte chemoattractant protein-1 [MCP-1]) and increased messenger RNA (mRNA) expression of the pleiotropic and angiogenic markers interleukin-6 (*IL-6*) and vascular endothelial growth factor-A (*VEGF*), respectively. Ionic osmolytes also demonstrated a greater level of change compared to the nonionic treatments, with mRNA levels of *IL-6* the most significantly affected. M(IFN) exposed to K^+ exhibited the lowest levels of NOS-2 and MCP-1, and this ion limited IL-6 release induced by osmolarity.
Conclusion: Cumulatively, these data suggest that osmolyte composition, ionic strength, and osmolarity are all parameters that can influence therapeutic outcomes. Future work is necessary to further decouple and mechanistically understand the influence that these biophysical parameters have on cell biology, including their impact on other macrophage functions, intracellular osmolyte composition, and cellular and organellular membrane potentials.

Keywords: inflammation, macrophages, 3D culture, ions, hyperosmolarity, membrane voltage potential

Introduction

A CHRONICALLY ALTERED immune system and local tissue immune-cell landscape are relevant in a broad range of contexts and diseases, including long-term responses to foreign bodies (e.g., implanted biomaterials), osteoarthritis, cancer, and atherosclerosis.[1–4] Macrophages, plastic myeloid immune cells of the innate immune system, are a primary communicator of changes in the local cellular environment whose roles encompass both pro-inflammatory debris or foreign body clearance, as well as inflammation resolution and wound healing. Controlling or modifying the behavior of macrophages or other immune responders is attractive toward the treatment of many diseases. In this regard, approaches based on modulation of biophysical parameters through injection of solutions with varying osmolyte composition and/or osmolarity have emerged in distinct research groups as simple, scalable, cheap, and effective treatments in a wide variety of contexts, including joint disease, asthma, traumatic brain injury, cancer, foreign body response, and atherosclerosis.[5–13] Our long-term goal is to integrate the knowledge from these approaches to enable

[1]Department of Biomedical Engineering, Rensselaer Polytechnic Institute, Troy, New York.
[2]Department of Biomedical Engineering, Tufts University, Medford, Massachusetts.
[3]Department of Biology, Allen Discovery Center at Tufts University, Tufts University, Medford, Massachusetts.

finer tuning of, and improved justification for, the composition of these therapies.

Significant prior work with macrophages *in vitro* has highlighted not only the specificity with which a given biophysical input can alter cellular function but also the complexities and redundancies that surround how these alterations are incurred. For example, studies stemming from the finding that tissues can retain sodium ions (Na^+) have shown that this microenvironmental cue can trigger macrophage chemotaxis[14] and shape a macrophage's function to either promote inflammation/host defense[15–17] or reduce would healing,[18] while others have suggested the opposite effect.[19] In another context, researchers have been interested in understanding how a macrophage can sense tissue osmolarity, showing this osmotic stimulus to be potently pro-inflammatory *in vitro* and *in vivo*.[16] However, no specific mechanism could be determined to show how the cell was sensing or transducing this osmolarity, a fact they attributed to significant functional redundancy and compensation.[16] Other ions, such as potassium (K^+), are emerging in specific microenvironments with seemingly opposite effects from that of Na^+.[20–24] For example, increasing extracellular K^+ is a stimulus that suppresses the (NOD)-like receptor protein 3 (NLRP3) inflammasome and the production of the prototypical cytokine interleukin-1-beta (IL-1β).[25,26] At a fundamental level, ions are not only chemical messengers that can bind to proteins and affect enzymatic activity but also electrical ones with their net balance across a membrane forming a dynamically changing voltage potential. Modulation of gradients of a cell's transmembrane voltage potential (V_{mem}) is investigated for their potential capacity to control tissue and organ level effects such as wound healing and regeneration or tissue patterning,[27,28] approaches which could have wide-reaching benefits. On a cellular basis, V_{mem} has been found to be a potent regulator of cell state, controlling an array of cellular functions.[26,27,29–32]

However, while it is likely that all of the aforementioned parameters influence macrophage functions, generally these factors have been pursued separately or in isolation. They have been therefore associated with a range of experimental design restrictions. Usually studies focus on the regulation of cell behaviors due to a specific biophysical parameter like osmolarity or a given ion for a single metric and/or time point.[17,19] In other instances, transmembrane voltage potentials have been ruled out or implicated as mechanistic drivers of features of cell phenotype based on experiments performed with noncalibrated, semiquantitative Nernstian-like dyes to assess voltage parameters.[21,33,34] Thus, even in the most controlled contexts (*in vitro* cell culture), many fundamental questions persist about if and how any of the above parameters, particularly when interacting, influence macrophage/cell biology. While the previously listed applications support the manipulation of these parameters as therapies, a deeper knowledge and integrated framework for how each factor may alter a macrophage's function would enable improvement or repurposing in contexts. The overarching hypothesis of this work is that biophysical factors, including ionic species, ionic strength, osmolarity, and V_{mem}, are determinants of cell states and functions. Specifically, we propose that K^+ treatment, either through its effects as an ion or as a chemical, is a unique anti-inflammatory and pro-resolving signal.

Previously, we have demonstrated that extracellular hyperosmolar (80 mM) K^+ gluconate (KG) elicits suppression of pro-inflammatory features of chondrocytes and macrophages.[35–38] While the emerging data for T cells and cancer seem clearer, whether potassium-based treatments have effects on activated macrophages separate from the well-known effects on the NLRP3 inflammasome and IL-1β is unknown. This is critical because macrophages have a dynamic secretome outside of a single cytokine,[39] all of which likely have distinct immunological consequences.

In this present study, our goals were twofold: (1) to provide additional evidence for hyperosmolar K^+ to exert a unique, potentially anti-inflammatory or immunosuppressive effect on macrophages and (2) to begin to decouple the influence that osmolyte composition, ionic strength, osmolarity, and V_{mem} may impart on macrophage cell biology. Extending our previous work,[32] here we more comprehensively examine the capacity of several hyperosmolar treatments to alter the phenotype of a pro-inflammatory macrophage subtype. We provide important steps toward achieving a deeper understanding of the specifics for how biophysical signals, including ionic species, ionic strength, osmolarity, and V_{mem}, influence distinct aspects of macrophage functions.

Materials and Methods

Polymer synthesis, functionalization, and hydrogel fabrication

Poly(ethylene glycol) diacrylate (PEGDA) was synthesized from PEG-diol (6 kDa; Sigma–Aldrich) at ~99% acrylation as reported previously.[40] In addition, the cell adhesion peptide NH_2-Arg-Gly-Asp-Ser-COOH (RGDS; American Peptide) was reacted with acryloyl-PEG-succinimidyl valeric acid (ACRL-PEG-SVA, 3.4 kDa; Laysan Bio) at the molar ratio of 1:1. Resulting ACRL-PEG-RGDS was purified by dialysis and then lyophilized and stored at −80°C until use. Hydrogels were fabricated from photo-crosslinking of a precursor solution containing 100 mg mL^{-1} 6 kDa PEGDA (97% acrylate), 1 mM ACRL-PEG-RGDS in phosphate-buffered saline (PBS; Gibco), and 1 vol% of the photoinitiator Irgacure (262 mg mL^{-1} in 70% ethanol, Sigma Aldrich). The precursor solution underwent sterilization and endotoxin removal using 0.2 μm Acrodisc® Units with Mustang® E Membrane filter (Pall Life Science). The molecular weight, concentration, and RGDS concentration of the PEGDA hydrogels were selected based on previous work.[35,40]

Cell culture and encapsulation

Cryopreserved RAW 264.7 (ATCC) macrophages, a murine macrophage cell line, were thawed and expanded in monolayer and maintained at 37°C/5% CO_2 in high glucose Dulbecco's modified Eagle's medium (Cellgro) supplemented with 10% fetal bovine serum (Hyclone), 100 U/mL penicillin, and 100 μg/mL streptomycin (Gibco). This cell line was chosen because it lacks the apoptotic speck-like protein containing a caspase recruitment domain required for NLRP3 inflammasome formation and thus the ability to produce IL-1β through this canonical mechanism,[41] yet exhibits a robust response to classical activators. This allows for NLRP3 inflammasome independent mechanisms to be studied *in vitro*. Despite differences between human

monocyte-derived macrophages and RAW 264.7 cells, many studies have demonstrated their ability to recapitulate key features of both classically and alternatively activated human monocyte derived macrophages.[42–48]

Cell encapsulation was performed as previously described.[36] Briefly, hydrogel discs were casted in a 48-well plate (BD Falcon) with 200 μL of cell suspension ($\sim 5 \times 10^6$ cells mL^{-1}) per well and exposed to long wavelength UV light for 6 min for polymerization (Spectroline, ~ 10 mW-cm^2, 365 nm). The three-dimensional (3D) encapsulation of macrophages was selected over conventional two-dimensional (2D) culture to restrict cell proliferation and protein deposition, minimizing the influence of potentially confounding factors on macrophage phenotype.[49–51]

After 24 h of acclimation to the 3D environment and activation of cells with 75 ng/mL interferon-gamma (IFNγ; R&D Systems), discs were placed in media with IFNγ supplemented with different treatments, including 80 mM K^+ gluconate, 80 mM Na^+ gluconate, or 160 mM sucrose (all from Sigma) for 24 h, selected in accordance with literature.[35–38,52–55] At the end point, hydrogels were washed in Dulbecco's PBS for 5 min, harvested, flash frozen in liquid nitrogen, and stored at −80°C. Media samples were also collected and frozen for further analysis. Encapsulated and activated macrophage samples are denoted hereafter as M(Cntl), M(IFN), M(KG), M(NaG), and M(Suc). All salt subsets received IFNγ stimulation. M(Cntl) are control encapsulated macrophages without activation.

Messenger RNA isolation, reverse transcriptase quantitative chain reaction, and total DNA quantification

Sample messenger RNA (mRNA) was isolated from gel lysates using Dynabeads™ mRNA DIRECT Kit (Invitrogen) as previously described.[37] During the extraction, protein and DNA are kept for future analysis separate from isolated mRNA. Reverse transcriptase quantitative chain reaction was performed to quantitatively evaluate mRNA expression levels across experimental groups as previously described.[35] A StepOne Real-Time PCR system (Life Technologies) with the SuperScript III Platinum One-Step reverse transcription quantitative polymerase chain reaction (RT-qPCR) Kit was utilized according to the manufacturer's instructions. Validated primers were purchased from OriGene, Eurofins Genomics, and Operon, and primer sequences are included (Supplementary Table S1). Gene amplification over 40 cycles was monitored by measuring the change in SYBR Green fluorescence, with ROX dye serving as a passive reference. Gene expression was normalized to three reference genes (*GAPDH*, *β-actin*, and *RPL32*), as described previously,[35,36] and is presented as relative fold change compared to M(IFN). Analysis was conducted using the ΔΔCt method for the estimation of relative gene expression.[56] Appropriate amplification product was verified by melting temperature analysis. Total DNA was measured by Quant-iT™ PicoGreen dsDNA Assay (Invitrogen), following the manufacturer's protocol. DNA levels were utilized for assessing cell viability and normalization of protein levels on a per cell basis during end point analyses.

Western blot and multiplex immunoassays

Western blots and multiplex immunoassays were used to measure protein expression of intracellular and secreted phenotypic-associated protein markers from the gel lysate and conditioned media, respectively. Western blots were performed using a 12–12.5% sodium dodecyl sulfate–polyacrylamide gel electrophoresis (SDS-PAGE) gel loaded with denatured and reduced protein samples, as described previously.[40] Protein expression was then quantified using integrated band densitometry. Resulting band intensities for nitric oxide synthase-2 (NOS-2) were normalized to three metrics to improve robustness of results: (1) beta-actin, (2) GAPDH, and (3) sample DNA content. Each lane was loaded with equivalent DNA amounts. A full list of primary antibodies used in western blots is provided (Supplementary Table S2).

Expression of secreted proteins (tumor necrosis factor-alpha [TNFα], monocyte chemoattractant protein-1 [MCP-1], vascular endothelial growth factor-A [VEGF], and interleukin [IL]-10, -13, -4, -1β, and -6) was measured from media samples using a Murine Magnetic Bead Analyte Kit (EMD Millipore). Median fluorescence intensity of each analyte was read using a MAGPIX system (Luminex). Concentrations of proteins of interest were calculated using the median fluorescence intensity and the standard curve of each analyte, as previously described.[57] Resulting protein concentrations from multiplex analyses were normalized by their respective sample DNA content.

Fluorescent measurement of membrane potential using DiSBAC$_2$(3)

Bis-(1,3-diethylthiobarbituric acid) trimethine oxonol (DiSBAC$_2$(3); Invitrogen) an anionic, fluorescent, voltage sensitive dye, was utilized to measure relative changes of cell membrane potential. Relative measurement with a dye was chosen due to limitations of patch-clamp electrophysiology[58] and difficulty in absolute calibration of the dyes.[59] DiSBAC$_2$(3) accumulates in the cytoplasm of depolarized cells with the fluorescence intensity increasing in response to the degree of depolarization. RAW 264.7 macrophages were incubated in Hank's buffered salt solution (HBSS; Invitrogen) with 0.5 μM of DiSBAC$_2$(3) (Sigma) for 30 min at 37°C before image acquisition.[55] Images were acquired with a Zeiss LSM 510 confocal microscope equipped with a LD Plan-Neofluar 40×/0.60 corr objective. DiSBAC$_2$(3) was excited at 543 nm with a HeNe1 laser (1%, to prevent photobleaching), and the emission was collected through a 560–615 nm barrier filter. Images were captured before and 10 min after addition of the treatments (80 mM KG, 80 mM NaG, 160 mM Suc, or a HBSS control) and then further processed for the percent change of MFI per cell upon stimulation. A pre–post comparison was conducted to control for unequal dye loading and dye efflux. Images were first de-noised with a median filter (5-pixel radius) to preserve edges for ROI selection and then background subtracted with a rolling ball filter (100-pixel radius). Cells were manually traced using the ROI manager, and the resulting percent change of MFI before and after simulation was calculated per cell. ImageJ/FIJI was utilized for all processing.

Statistical analyses

All results are reported as the mean ± standard error of the mean. Means were compared using either an unpaired

t-test or *post hoc* testing ($n = 4$–15 independent hydrogels or $n = 26$–36 cells per group from either two to four independent experiments, as denoted in figure legends) depending on whether two or more groups were being compared. Homogeneity of variances was assessed with Levene's test. If equal variances were verified, then Tukey's *post hoc* test was performed, otherwise the Games-Howell *post hoc* test was utilized. For all analyses, a p-value <0.05 was considered significant, and SPSS software was utilized.

Results

IFNγ but not Lipopolysaccharide activates macrophages in 3D PEGDA hydrogels

Much of the mechanistic work to understand how cells can rewire metabolism to support their pro-inflammatory, functional attributes has been performed with lipopolysaccharide (LPS) as the stimulant. To improve the fidelity of our results with literature,[60–63] we started by attempting to study this macrophage state in our 3D culture model system. However, none of the analyzed markers between M(Cntl) and M(LPS) was different (Fig. 1A), likely due to the micellular nature of LPS—forming aggregates too large to penetrate the PEGDA hydrogel network. Therefore, we reverted to IFNγ stimulation[36] to generate a pro-inflammatory macrophage subtype in the encapsulated 3D environment. We confirmed M(IFN) through assessment of markers commonly associated with macrophage functions—*TNFα*, *IL-6*, and *VEGF-A* (Fig. 1B and Supplementary Fig. S1). Specifically, relative to M(Cntl), M(IFN) exhibited significantly higher mRNA expression of TNFα (~10-fold $p < 0.0005$) and IL-6 (~11-fold $p < 0.0005$), but no difference with respect to *VEGF* mRNA levels (Fig. 1B). These data demonstrate a classically activated polarization state in 3D PEGDA hydrogels sufficient for the purpose of investigating the effects of different hyperosmolar treatments on M(IFN).

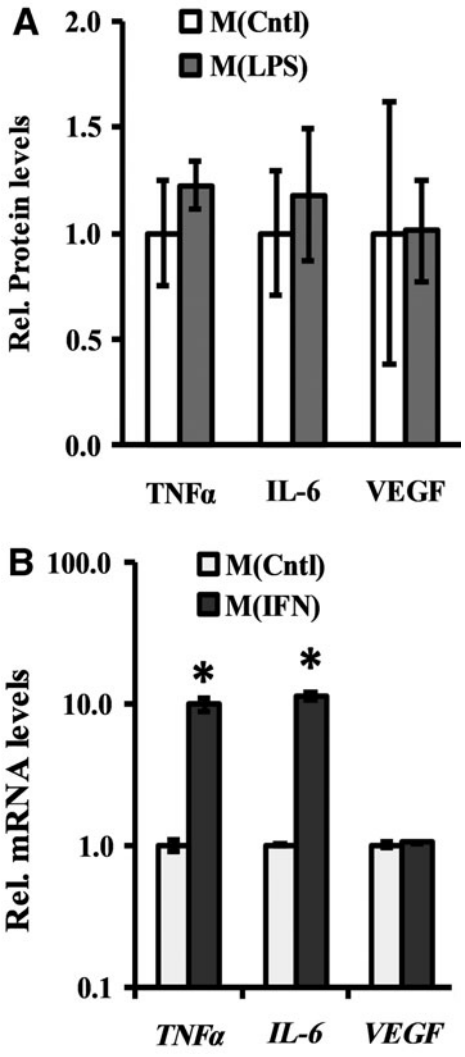

FIG. 1. Comparison of macrophage activation protocols in PEGDA hydrogels. Phenotype assessments were performed on PEGDA encapsulated RAW 264.7 cells after 24 h stimulation with either **(A)** 1 μg/mL LPS, M(LPS), or **(B)** 75 ng/mL IFNγ, M(IFN). Data are shown relative to nonactivated M(Cntl). Results are from four independent hydrogels ($n = 4$) for each condition and are representative of two independent experiments. *Statistically different from M(Cntl) by an unpaired *t*-test assuming equal variances, $p < 0.05$. IFN, interferon; IL, interleukin; LPS, lipopolysaccharide; PEGDA, poly(ethylene glycol) diacrylate; TNFα, tumor necrosis factor-alpha; VEGF, vascular endothelial growth factor A.

Osmolarity and K^+ impart specific and marker-dependent effects on M(IFN) at the intracellular protein level

After verification of M(IFN), we aimed to assess the ability of hyperosmolar K^+ to suppress M(IFN) activation and decouple these effects from confounding factors, including osmolarity and ionic strength (Fig. 2). We introduced several experimental groups to control for these factors, including: (1) 160 mM sucrose as a nonionic osmolarity control and (2) 80 mM Na^+ gluconate as a control for both effects of ionic strength and the gluconate anion. First, we assessed NOS-2 protein from the gel lysates, one of the canonical markers of M(IFN) that we have previously shown to be affected by treatment with 80 mM KG.[36] More broadly, NOS-2 and nitric oxide have been a focus and potential integration point for emerging mechanistic understandings of the ties between metabolism, mitochondria, and inflammation in the murine macrophage model system.[64–68]

Representative western blot images for NOS-2 and the normalizing proteins GAPDH and β-actin in addition to equal loading of lanes based on DNA levels are shown in Figure 3A, and cell viability is shown in Supplementary Figure S2. Relative to M(IFN), all groups with elevated osmolarity (independent of a specific type of osmolyte) did not induce cell death (Supplementary Fig. S2) and showed a significant reduction in NOS-2 levels after 24 h of treatment (>2.0-fold, $p < 0.0005$; Fig. 3B). This effect was more prominent with potassium treatment. Specifically, M(KG) exhibited significantly lower NOS-2 levels relative to the gluconate and ionic strength control M(NaG) (~3.8-fold, $p = 0.008$), a difference not noted with the nonionic osmolyte control M(Suc), which was elevated relative to M(NaG) (~3.0-fold, $p = 0.128$; Fig. 3B). Cumulatively, these data suggest that osmolarity and ionic species (K^+) affect M(IFN) from a NOS-2 protein perspective.

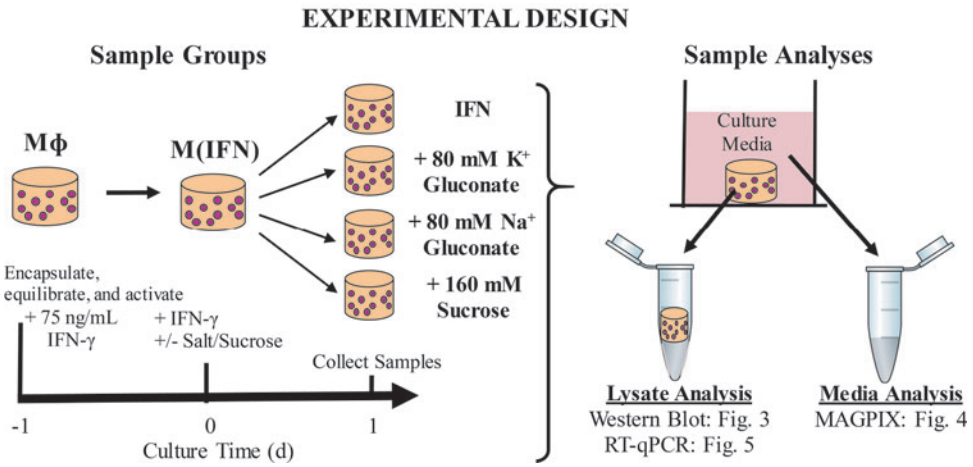

FIG. 2. Experimental design for determining the influence of hyperosmolar solutions of differing osmolyte composition on the protein and gene level phenotype of M(IFN) cultured in PEGDA hydrogels. Cells were exposed to treatments for 1 day before sample analyses. Sodium gluconate (80 mM) was included to control for effects of ionic strength and the gluconate ion. Sucrose (160 mM) was included as a nonionic osmolyte control. IFNγ, interferon-gamma; RT-qPCR, reverse transcriptase quantitative polymerase chain reaction.

Osmolarity and K^+ impart specific and marker-dependent effects on secreted proteins

Given the increasing prominence of ionic species-specific effects on immune cells, we performed additional analyses on secreted factors from our cultures since these represent distinct facets of a macrophage's function. Using MAGPIX multiplex immunoassays, we quantitatively profiled the levels of several secreted proteins—TNFα, MCP-1, IL-6, and VEGF, and normalized these concentrations to cell DNA assessments and further to M(IFN) (Fig. 4). Other analytes that we profiled included IL-1β, IL-4, IL-10, IL12-p40, and IL-13, none of which were consistently detected above the lowest standard throughout our experiments (3.2 pg/mL; data not shown). With respect to detected proteins, TNFα and VEGF levels were unaffected by osmolyte treatment (Fig. 4). However, in a similar manner with that of NOS-2 (Fig. 2B), all three hyperosmolar treatments significantly reduced MCP-1 levels (>1.9-fold, $p < 0.0005$), with M(KG), but not M(NaG), showing a further reduction in MCP-1 relative to M(Suc) (>2.3-fold, $p < 0.006$; Fig. 4). Moreover, in contrast to all other markers, M(NaG) had a unique effect on the pleiotropic cytokine IL-6, elevating the secreted levels of the protein relative to both M(IFN) (1.8-fold, $p < 0.0005$) and M(KG) (2-fold, $p < 0.008$), effects that were not noticed in M(Suc) (Fig. 4). Cumulatively, these data suggest that both osmolarity and K^+ are also capable of affecting macrophage biology by regulating secreted factors in a marker-dependent manner (e.g., osmolarity only affecting MCP-1; K^+ further suppressing MCP-1 and preventing the increase in IL-6).

Osmolarity, ionic strength, and K^+ impart specific and marker-dependent effects on gene expression

In addition to protein metrics that were performed 24 h after stimulation, we assessed macrophage phenotype at the mRNA level to gain insight into potential future cell behavior

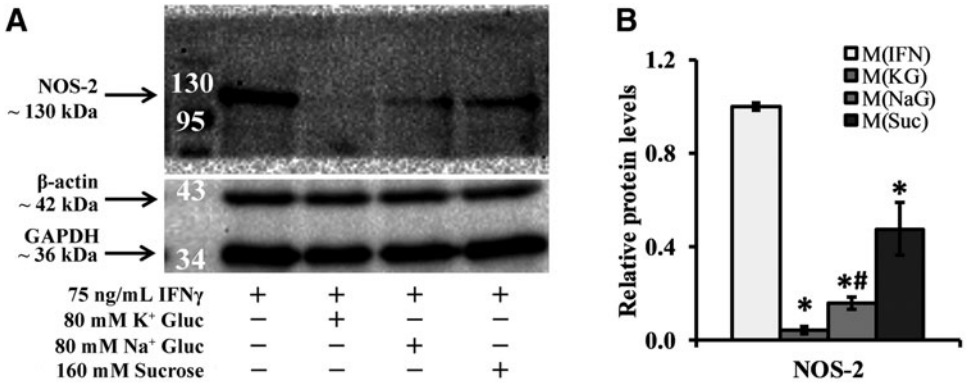

FIG. 3. **(A)** Representative western blot images of NOS-2 (130 kDa) and normalizing proteins β-actin and GAPDH (42 and 36 kDa, respectively) for all treatment groups. Equal amounts of DNA for each sample were loaded per lane. **(B)** Abundance of NOS-2 across different hyperosmolar treatments shown relative to M(IFN). Results are from three independent experiments with $n = 9$, 9, 8, and 4 hydrogels for M(IFN), M(KG), M(NaG), and M(Suc), respectively. *Statistically different from M(IFN) and #statistically different from M(KG), assessed by a Games-Howell *post hoc* test, $p < 0.05$. NOS-2, nitric oxide synthase-2.

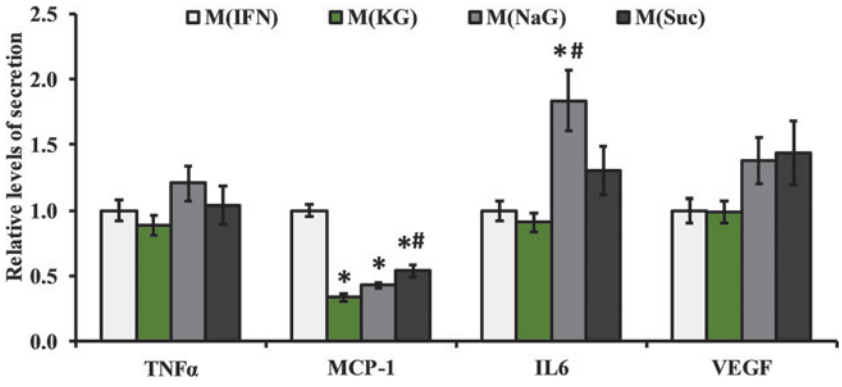

FIG. 4. Levels of secreted proteins assessed from media of 3D hydrogel cultures with different hyperosmolar treatments shown relative to M(IFN). Results are from four independent experiments with $n = 15$, 15, 12, and 8 hydrogels for M(IFN), M(KG), M(NaG), and M(Suc), respectively. *Statistically different from M(IFN) and #statistically different from M(KG), assessed by either a Tukey (TNFα) or Games-howell (IL-6, MCP-1, VEGF) *post hoc* test, $p < 0.05$. MCP-1, monocyte chemoattractant protein-1.

and as a way to further identify biophysical regulation of cell biology. Figure 5 displays the relative mRNA levels of the targets we investigated. In terms of osmolarity, all hyperosmolar treatments exhibited reduced mRNA expression of pro-inflammatory markers *NOS-2* (>1.4-fold, $p < 0.001$) and *MCP-1*(>4.2-fold, $p < 0.001$), and *TNFα* (>1.7-fold), although this fell below statistical significance for M(KG) (4.6-fold, $p = 0.059$; Fig. 5A). In addition to the general effect of osmolarity, treatment with 80 mM KG further suppressed mRNA levels of *NOS-2* (~2.6-fold, $p < 0.0005$), *MCP-1* (~2.5-fold, $p < 0.001$), and *TNFα* (~2.6-fold, $p < 0.023$) relative to both M(NaG) and M(Suc) groups (Fig. 5A). Finally, no differences between M(NaG) and M(Suc) were observed (Fig. 5A).

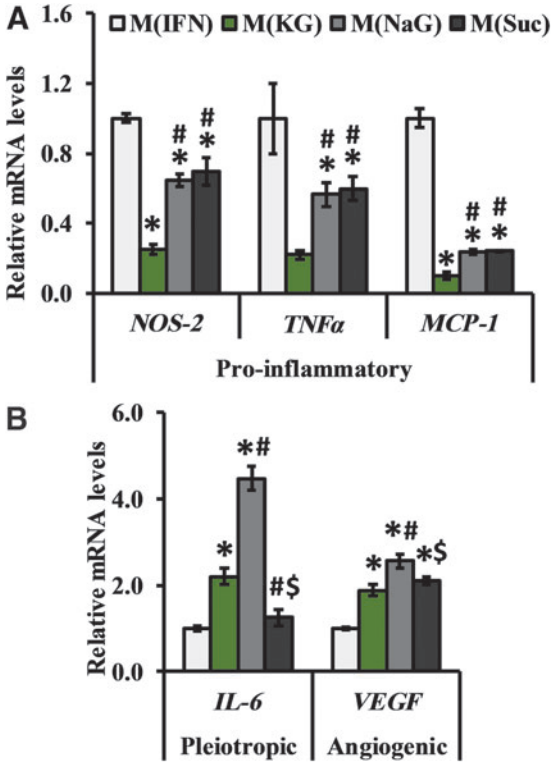

FIG. 5. Relative mRNA expression levels of **(A)** pro-inflammatory and **(B)** pleiotropic and angiogenic markers under the different treatment conditions. Relative mRNA levels for target transcripts were calculated utilizing a combination of *GAPDH*, *β-act*, and *RPL32* as reference genes. Results are from four independent hydrogels ($n = 4$) for each condition and are representative of two independent experiments. *Statistically different from M(IFN), #statistically different from M(KG), and $statistically different from M(NaG), assessed by either a Tukey (*NOS-2*, *VEGF-A*, *IL-6*) or Games-Howell (*TNFα*, *MCP-1*) *post hoc* test, $p < 0.05$. mRNA, messenger RNA.

In contrast to pro-inflammatory markers, mRNA levels for other proteins such as *IL-6* and *VEGF-A* were affected by osmolarity, ionic strength, and osmolyte composition in a more complex manner (Fig. 5B). For example, relative to M(IFN), solutions with shared ionic strength, but not M(Suc), had significantly elevated levels of *IL-6* (>2.2-fold, $p < 0.001$), but all macrophages that were exposed to elevated osmolarity exhibited higher mRNA levels of the angiogenic protein *VEGF-A* (>1.9-fold, $p < 0.0005$; Fig. 5B). Notably, M(NaG) had significantly higher *VEGF-A* (~2.6-fold, $p < 0.0005$) and *IL-6* (~4.5-fold, $p < 0.0005$) mRNA expression relative to M(KG) and M(Suc) (Fig. 5B).

Cumulatively, these data suggest the following: (1) hyperosmolar solutions suppress key markers of inflammation and promote markers of wound healing; however, (2) ionic osmolytes demonstrated more pronounced immunomodulatory effects compared to sucrose, and (3) there is a K^+ specific effect on all assessed pro-inflammatory markers.

Each hyperosmolar composition elicits differential effects on membrane potential

To gain an initial sense of potential mechanisms by which the different hyperosmolar treatments impart their effects, macrophage membrane potential was measured semi-quantitatively using a fluorescent voltage sensitive dye, $DiSBAC_2(3)$. Essentially, by taking fluorescence measurements pre- and postperturbation with the different osmolyte treatments (Supplementary Fig. S3), the relative changes in membrane potential can be quantified (Fig. 6), with an increase or decrease in mean fluorescence intensity (MFI) signifying depolarization or hyperpolarization of a cell, respectively. Relative to control macrophages that received addition of HBSS to control for liquid handling, addition of KG significantly depolarized (24.6% increase, $p < 0.0005$), NaG imparted no effect (2.2% decrease, $p < 0.998$), and sucrose significantly hyperpolarized (39% decrease, $p < 0.0005$) V_{mem} (Fig. 6). Voltage imaging suggests that each osmolyte may impart distinct voltage profiles to macrophages.

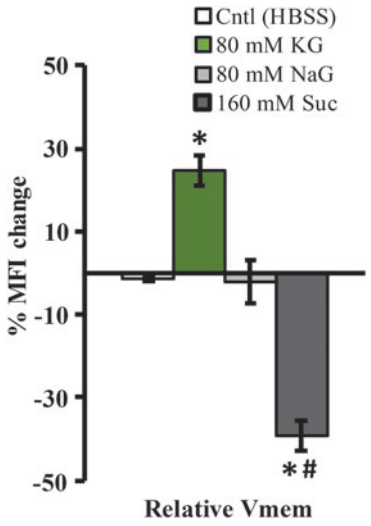

FIG. 6. Relative V_{mem} measurements assessed utilizing confocal microscopy and a Nernstian-like fluorescent dye—$DiSBAC_2(3)$. Mean fluorescence intensity was compared on a per-cell basis pre- and post-treatment after 10 min of exposure. The sample size (number of cells) for Cntl, KG, NaG, and Suc groups was $n = 36$, 26, 36, and 32, respectively. Data are representative from three independent experiments. *Statistically different from M(IFN) and #statistically different from M(KG), assessed by a Games-Howell *post hoc* test, $p < 0.05$. $DiSBAC_2(3)$, Bis-(l,3-diethylthiobarbituric acid) trimethine oxonol; MFI, mean fluorescence intensity.

Discussion

The objectives of this study were to: (1) provide evidence for K^+ to exert a unique, potentially anti-inflammatory or immunosuppressive effect on macrophages, and (2) more broadly begin to decouple the influence that osmolyte composition, ionic strength, osmolarity, and V_{mem} may exert on cell functions. Macrophages were encapsulated in 3D PEG-DA hydrogels,[36] activated with a pro-inflammatory stimulus (IFNγ) and subsequently exposed to KG, NaG, and Suc (all $\sim$160 mOsm hyperosmolar) and assessed utilizing several intracellular (gene and protein) and extracellular (protein) metrics (Fig. 2). Balancing the feasibility of the experimental design with respect to number of experimental groups (dosages and different compositions), time points, and end point analyses, the design was focused on isolating effects due to K^+ or osmolarity, with some overlap in terms of metrics for ionic strength.

We focused on K^+ to be consistent with our previous work[35–37] and that of others for other cell types[21,69] and utilized the RAW 264.7 macrophage cell line to study the broader impact of this ion independent from its well-studied effects on the NLRP3 inflammasome.[25,26] Our results indicated that M(KG) exhibited the strongest suppression of NOS-2 production (Fig. 3B) and MCP-1 release (Fig. 4) while also limiting or preventing IL-6 secretion elicited by M(NaG) and M(Suc). It is clear that K^+ was able to specifically alter the functional status of M(IFN), supporting our initial work.[35–37] In addition to protein level assays, mRNA assessments indicated a unique role for K^+ with respect to inhibition of pro-inflammatory markers ($\downarrow$*NOS-2*, *MCP-1*, and *TNFα*) relative to all other groups (Fig. 5). It is possible that our early time point for protein level assessments precluded the ability to see clearer effects of K^+ at the protein level for TNFα. This warrants further investigation.

Cumulatively, these protein- and gene-level data are important for both practical and scientific reasons. First, they suggest that extended-release strategies utilizing K^+ may exert different effects from that of a simple injection, offering more opportunities for therapies. Second, the NOS-2 data are particularly interesting from an immunometabolic perspective, aligning with several lines of evidence pointing toward K^+-specific promotion of immunosuppression and cell quiescence through mitochondrial-based mechanisms.[21–23,69] This is perhaps not surprising when placed in an evolutionary context, with the first ''protocells'' believed to be formed in a potassium-rich environment[70–72] and with the emerging data supporting the recognition of this ion by our immune system as ''self.''[21,69] Importantly, our data with RAW 264.7 macrophages support the less appreciated notion that K^+ can regulate macrophage metabolism and function through mechanisms independent of NLRP3 inflammasome inhibition, while still remaining similar to primary human monocyte derived macrophages with respect to many other functional attributes.[42–48]

In terms of osmolarity, we found that all three hyperosmolar treatments resulted in significant decreases in both protein and mRNA expression of pro-inflammatory markers NOS-2 (Figs. 3 and 5A) and MCP-1 (Figs. 4 and 5A) and increases in mRNA levels for the pleiotropic and angiogenic markers *IL-6* and *VEGF*, respectively (Fig. 5B). These anti-inflammatory findings generally agree with the therapeutic applications of hyperosmolar treatments[5–13] but contrast with other work.[15,16,73–75] There are several possible experimental design explanations for these discrepancies, including differences in: (1) cell or tissue type,[35,76] (2) culture dimensionality (2D vs. 3D),[77–80] (3) concentration of osmotic solution,[16,17,74–76,81] and (4) end point metrics and timing.[16,74–76,81]

Regardless of the above discrepancies and keeping shared phenotypic effects across all treatments in mind, we performed confocal imaging with $DiSBAC_2(3)$ to gain a deeper mechanistic understanding between the relationship of cell function and V_{mem}. We reasoned that if all three treatments exhibited similar effects on voltage, then the likelihood that this specific biophysical parameter was mechanistically involved would be high. In contrast, we found that each hyperosmolar solution evoked distinct responses: 80 mM KG depolarized (25% increase), 160 mM sucrose hyperpolarized (39% decrease), and 80 mM NaG did not alter population level V_{mem} (Fig. 6). The fact that all three osmolytes showed the same direction and similar magnitude of change for NOS-2, TNFα, MCP-1, IL-6, and VEGF, yet all showed distinct effects on V_{mem}, suggests that V_{mem} is not the major determinant of any of these aspects of a macrophage's function. However, we cannot definitively eliminate plasma membrane voltage gradients as an important transduction parameter, due to the semiquantitative nature of non-calibrated, Nernstian-like dyes and the fact that we only assessed voltages at a single acute time point in 2D cultures. All of above data and observations both agree and disagree with previous work done with extracellular K^+ and T cell effector functions. Examples of this in our results include the agreement of our strong evidence for K^+ specificity, but, contrarily,

we are less conclusive with respect to definitively claiming independence from V_{mem} because of dye and experimental design considerations noted above.[21]

Outside of immunology, hyperpolarization of V_{mem} shows promise as a potential therapy in the context of cancer[82–86]; thus our results suggest that sucrose could be a relatively inexpensive and easy way to induce such a hyperpolarizing effect. Future work will continue to address the gaps in knowledge surrounding the degree to which cells can sense and respond to biophysical cues, and definitive answers will likely require currently nonexistent but ever increasing, multiplexed methods to quantitatively monitor electrical, ionic, and biophysical properties in many cells simultaneously with time.[59,87–89]

Finally, both the ionic osmolytes shared the following effects relative to the nonionic M(Suc) groups: (1) promotion of *IL-6* mRNA levels (Fig. 5B), (2) suppression of NOS-2 (Fig. 2B), and (3) inhibition of secreted MCP-1 (Fig. 4), although not achieving statistical significance for NOS-2 and MCP-1. These data demonstrate an independent role for ionic strength (separate from osmolarity and composition) in affecting macrophage functions, consistent with reports in other fields.[90–92] It is difficult to compare the specifics of our results to literature because relative to osmolarity, the ionic strength of a solution has received little attention. For example, the words ''ionic strength'' often cannot be found within a body of work pertaining to hyperosmolarity, inflammation, and macrophages,[16,19,76,81,93] many of which utilize ionic osmolytes. Unraveling the subtleties between ionic strength and osmolarity will be difficult for many reasons, but our results support revisiting and potentially redesigning hyperosmolar therapies that currently do not take this parameter into account, at least overtly.[5,6,94]

Some limitations must be considered when interpreting the results reported herein. Our study was largely proof-of-concept in nature, so we were limited with respect to many of the types of experimental groups included and end point analyses assessed. This affected our ability to interpret some findings (e.g., differences between M(NaG) and M(KG) when both are also different from M(Suc) cannot currently be attributed to Na^+ or K^+). Our study design also may have hampered comparison of our results to the literature utilizing different macrophage stimulants, dosages of osmolytes, or investigating different cytokines. Second, the broader extrapolation of our results to a tissue-level response to these stimuli may be difficult because of the experimental system utilized (*in vitro* culture with a cell line). While we consider the RAW 264.7 cell line and 3D culture as strengths for this study, future work will include additional experimental groups, a more exhaustive list of secreted factor functional assessments, primary human and mouse cell types, and quantitative *in vivo* models of inflammation.

Conclusions

To summarize, the relationship between biophysical parameters is intricate and complex. Our data demonstrate that osmolyte composition (effects observed in M(KG) but not M(NaG) or M(Suc)), osmolarity (similar effects elicited by all three hyperosmolar solutions), and ionic strength (effects noticed in both M(KG) and M(NaG) but not M(Suc)) impact macrophage biology in several distinct ways. Moreover, we provide initial data to suggest that the observed effects were not due to the impact these parameters have on V_{mem}. Future work that further decouples the impact of biophysical cues on cell biology, including more in-depth secretomic and metabolic characterizations, will be useful toward creating or improving upon hyperosmolar based therapies for a broad range of inflammation driven or relevant pathologies.

Author Confirmation Statement

J.E.-M. carried out conception and designed the experiments. J.E.-M. and H.C. performed experiments and data collection. J.E.-M. analyzed and interpreted data. J.E.-M. and D.J.Y. wrote article. M.L., D.L.K., and M.S.H. revised and edited the article. All authors have reviewed and approved the article before submission.

The authors declare that the article has not been published, in press, or submitted elsewhere.

Author Disclosure Statement

J.E.-M. and M.S.H. have a patent related to this work (US Patent App. 16/285,348, 2019).

Funding Information

The authors thank the National Institutes of Health (P41 Resource Center on Tissue Engineering (P41EB002520) to D.L.K., Allen Discovery Center program through The Paul G. Allen Frontiers Group (12171), NIA R03AG064550 and NIA R03AG056168 to M.S.H., NIMH F32MH118678 to J.E.-M.).

Supplementary Material

Supplementary Table S1
Supplementary Table S2
Supplementary Figure S1
Supplementary Figure S2
Supplementary Figure S3

References

1. Robinson WH, Lepus CM, Wang Q, et al. Low-grade inflammation as a key mediator of the pathogenesis of osteoarthritis. Nat Rev Rheumatol 2016;12:580–592. DOI: 10.1038/nrrheum.2016.136
2. Klopfleisch R. Macrophage reaction against biomaterials in the mouse model—Phenotypes, functions and markers. Acta Biomater 2016;43:3–13. DOI: 10.1016/j.actbio.2016.07.003
3. Coussens LM, Werb Z. Inflammation and cancer. Nature 2002;420:860–867. DOI: 10.1038/nature01322.Inflammation
4. Gisterå A, Hansson GK. The immunology of atherosclerosis. Nat Rev Nephrol 2017;13:368–380. DOI: 10.1038/nrneph.2017.51
5. Capito NM, Smith MJ, Stoker AM, et al. Hyperosmolar irrigation compared with a standard solution in a canine shoulder arthroscopy model. J Shoulder Elb Surg 2015;24:1243–1248. DOI: 10.1016/j.jse.2014.12.027
6. Amin AK, Huntley JS, Simpson AHRW, et al. Increasing the osmolarity of joint irrigation solutions may avoid injury to cartilage: A pilot study. Clin Orthop Relat Res 2010;468:875–884. DOI: 10.1007/s11999-009-0983-7

7. Thompson CL, Yasmin H, Varone A, et al. Lithium chloride prevents interleukin-1β induced cartilage degradation and loss of mechanical properties. J Orthop Res 2015;33: 1552–1559. DOI: 10.1002/jor.22913
8. Bratton SL, Chestnut RM, Ghajar J, et al. II. Hyperosmolar therapy. J Neurotrauma 2007;24:14–20. DOI: 10.1089/neu .2007.9994
9. Boulet L, Legris C, Thibault L, et al. Comparative bronchial responses to hyperosmolar saline and methacholine in asthma. Thorax 1987;42:953–958.
10. Diringer MN. New trends in hyperosmolar therapy? Curr Opin Crit Care 2013;19:77–82. DOI: 10.1097/MCC.0b013e 32835eba30.New
11. Lee BS, Juthani RG, Healy AT, et al. Hyperosmolar and methotrexate therapy avoiding surgery in the acute presentation of primary central nervous system lymphoma. Surg Neurol Int 2014;5(SUPPL. 4):175–180. DOI: 10.4103/2152-7806.136741
12. Huang Y, Wu C, Zhang X, et al. Regulation of immune response by bioactive ions released from silicate bioceramics for bone regeneration. Acta Biomater 2018;66: 81–92. DOI: 10.1016/j.actbio.2017.08.044
13. Flexon P, Khan M, Luria MH. Effects of potassium chromate on atherosclerosis prevention and regression in rabbits. Atherosclerosis 1986;59:31–35. DOI: 10.1016/0021-9150(86) 90029-8
14. Müller S, Quast T, Schröder A, et al. Salt-dependent chemotaxis of macrophages. PLoS One 2013;8:2–10. DOI: 10.1371/journal.pone.0073439
15. Hucke S, Eschborn M, Liebmann M, et al. Sodium chloride promotes pro-inflammatory macrophage polarization thereby aggravating CNS autoimmunity. J Autoimmun 2016;67: 90–101. DOI: 10.1016/j.jaut.2015.11.001
16. Ip WKE, Medzhitov R. Macrophages monitor tissue osmolarity and induce inflammatory response through NLRP3 and NLRC4 inflammasome activation. Nat Commun 2015;6:6931. DOI: 10.1038/ncomms7931
17. Zhang WC, Zheng XJ, Du LJ, et al. High salt primes a specific activation state of macrophages, M(Na). Cell Res 2015;25:893–910. DOI: 10.1038/cr.2015.87
18. Binger KJ, Gebhardt M, Heinig M, et al. High salt reduces the activation of IL-4- and IL-13-stimulated macrophages. J Clin Invest 2015;125:4223–4238. DOI: 10.1172/ JCI80919
19. Amara S, Whalen M, Tiriveedhi V. High salt induces anti-inflammatory MΦ2-like phenotype in peripheral macrophages. Biochem Biophys Reports 2016;7:1–9. DOI: 10.1016/j.bbrep.2016.05.009
20. Bingel M, Lonnemann G, Dinarello CA, et al. Enhancement of in-vitro human interleukin-1 production by sodium acetate. Lancet 1987;329:14–16.
21. Eil R, Vodnala SK, Clever D, et al. Ionic immune suppression within the tumour microenvironment limits T cell effector function. Nature 2016;537:539–543. DOI: 10.1038/nature 19364
22. Chiang EY, Li T, Jeet S, et al. Potassium channels Kv1.3 and KCa3.1 cooperatively and compensatorily regulate antigen-specific memory T cell functions. Nat Commun 2017;8:14644. DOI: 10.1038/ncomms14644
23. Khalili H, Malik S, Ananthakrishnan AN, et al. Identification and characterization of a novel association between dietary potassium and risk of Crohn's disease and ulcerative colitis. Front Immunol 2016;7:554. DOI: 10.3389/ fimmu.2016.00554
24. Gianfrancesco MA, Dehairs J, L'homme L, et al. Saturated fatty acids induce NLRP3 activation in human macrophages through K+ efflux resulting from phospholipid saturation and Na, K-ATPase disruption. Biochim Biophys Acta Mol Cell Biol Lipids 2019;1864:1017–1030. DOI: 10.1016/j.bbalip.2019.04.001
25. Abderrazak A, Syrovets T, Couchie D, et al. NLRP3 inflammasome: From a danger signal sensor to a regulatory node of oxidative stress and inflammatory diseases. Redox Biol 2015;4:296–307. DOI: 10.1016/j.redox.2015 .01.008
26. Zhang Y, Rong H, Zhang FX, et al. A membrane potential- and calpain-dependent reversal of caspase-1 inhibition regulates canonical NLRP3 inflammasome. Cell Rep 2018; 24:2356–2369.e5. DOI: 10.1016/j.celrep.2018.07.098
27. Levin M, Stevenson CG. Regulation of cell behavior and tissue patterning by bioelectrical signals: Challenges and opportunities for biomedical engineering. Annu Rev Biomed Eng 2012;14:295–323. DOI: 10.1146/annurev-bioeng-071811-150114
28. Levin M. Reprogramming cells and tissue patterning via bioelectrical pathways: Molecular mechanisms and biomedical opportunities. Wiley Interdiscip Rev Syst Biol Med 2013;5:657–676. DOI: 10.1002/wsbm.1236
29. Sundelacruz S, Levin M, Kaplan DL. Role of membrane potential in the regulation of cell proliferation and differentiation. Stem Cell Rev Reports 2009;5:231–246. DOI: 10.1007/s12015-009-9080-2
30. Levin M. Molecular bioelectricity: How endogenous voltage potentials control cell behavior and instruct pattern regulation in vivo. Mol Biol Cell 2014;25:3835–3850. DOI: 10.1091/mbc.E13-12-0708
31. Kitagawa S, Johnston RBJ. Relationship between membrane potential changes and superoxide-releasing capacity in resident and activated mouse peritoneal macrophages. J Immunol 1985;135:3417–3423.
32. Li C, Levin M, Kaplan DL. Bioelectric modulation of macrophage polarization. Sci Rep 2016;6:21044. DOI: 10.1038/srep21044
33. Sanin DE, Matsushita M, Klein Geltink RI, et al. Mitochondrial membrane potential regulates nuclear gene expression in macrophages exposed to prostaglandin E2. Immunity 2018;49:1021–1033.e6. DOI: 10.1016/j .immuni.2018.10.011
34. Sukumar M, Liu J, Mehta GU, et al. Mitochondrial membrane potential identifies cells with enhanced stemness for cellular therapy. Cell Metab 2017;23:63–76. DOI: 10.1016/j.physbeh.2017.03.040
35. Erndt-Marino J, Trinkle E, Hahn MS. Hyperosmolar potassium (K+) treatment suppresses osteoarthritic chondrocyte catabolic and inflammatory protein production in a 3-dimensional in vitro model. Cartilage 2019;10:186–195. DOI: 10.1177/1947603517734028
36. Erndt-Marino J, Diaz-Rodriguez P, Hahn MS. Initial in vitro development of a potassium-based intra-articular injection for osteoarthritis. Tissue Eng Part A 2018;24: 1390–1392. DOI: 10.1089/ten.tea.2017.0390
37. Samavedi S, Diaz-Rodriguez P, Erndt-Marino JD, et al. A three-dimensional chondrocyte-macrophage coculture system to probe inflammation in experimental osteoarthritis. Tissue Eng Part A 2017;23:101–114. DOI: 10.1089/ ten.tea.2016.0007
38. Erndt-Marino JD, Hahn MS, inventors; Rensselaer Polytechnic Institute, assignee. Method of treatment via intra-

articular applications of potassium. United States patent US 2019/0262295A1. 2019.
39. Meissner F, Scheltema RA, Mollenkopf H, et al. Direct proteomic quantification of the secretome of activated immune cells. Science (80-) 2013;340:475–479.
40. Erndt-marino JD, Hahn MS. Probing the response of human osteoblasts following exposure to sympathetic neuron-like PC-12 cells in a 3D coculture model. Soc Biomater 2017; 105:984–990. DOI: 10.1002/jbm.a.35964
41. Bryan NB, Dorfleutner A, Kramer SJ, et al. Differential splicing of the apoptosis-associated speck like protein containing a caspase recruitment domain (ASC) regulates inflammasomes. J Inflamm 2010;7:23. DOI: 10.1186/1476-9255-7-23
42. Lin CY, Lin CJ, Chen KH, et al. Macrophage activation increases the invasive properties of hepatoma cells by destabilization of the adherens junction. FEBS Lett 2006;580: 3042–3050. DOI: 10.1016/j.febslet.2006.04.049
43. Liu CY, Xu JY, Shi XY, et al. M2-polarized tumor-associated macrophages promoted epithelial-mesenchymal transition in pancreatic cancer cells, partially through TLR4/IL-10 signaling pathway. Lab Investig 2013;93:844–854. DOI: 10.1038/labinvest.2013.69
44. Luo J-F, Shen X-Y, Lio CK, et al. Activation of Nrf2/HO-1 pathway by nardochinoid c inhibits inflammation and oxidative stress in lipopolysaccharide-stimulated macrophages. Front Pharmacol 2018;9:911. DOI: 10.3389/fphar .2018.00911
45. Li Q, Liu L, Zhang Q, et al. Interleukin-17 indirectly promotes M2 macrophage differentiation through stimulation of COX-2/PGE2 pathway in the cancer cells. Cancer Res Treat 2014;46:297–306.
46. Hao J, Hu Y, Li Y, et al. Involvement of JNK signaling in IL4-induced M2 macrophage polarization. Exp Cell Res 2017;357:155–162. DOI: 10.1016/j.yexcr.2017.05.010
47. Wang J, Wang R, Wang H, et al. Glucocorticoids suppress antimicrobial autophagy and nitric oxide production and facilitate mycobacterial survival in macrophages. Sci Rep 2017;7:982. DOI: 10.1038/s41598-017-01174-9
48. Chernikov O V, Wong W, Li L, et al. A GalNAc/Gal-specific lectin from the sea mussel Crenomytilus grayanus modulates immune response in macrophages and in mice. Sci Rep 2017;7:6315. DOI: 10.1038/s41598-017-06647-5
49. Gombotz WR, Guanghui W, Horbett TA, et al. Protein adsorption to poly(ethylene oxide) surfaces. J Biomed Mater Res 1991;25:1547–1562. DOI: 10.1002/jbm .820251211
50. Williams CG, Kim TK, Taboas A, et al. In vitro chondrogenesis of bone marrow-derived mesenchymal stem cells in a photopolymerizing hydrogel. Tissue Eng 2003;9: 679–688. DOI: 10.1089/107632703768247377
51. Nuttelman CR, Tripodi MC, Anseth KS. Synthetic hydrogel niches that promote hMSC viability. Matrix Biol 2005; 24:208–218. DOI: 10.1016/j.matbio.2005.03.004
52. Lan J-Y, Williams C, Levin M, et al. Depolarization of cellular resting membrane potential promotes neonatal cardiomyocyte proliferation in vitro. Cell Mol Bioeng 2014;7:432–445. DOI: 10.1007/s12195-014-0346-7
53. Sundelacruz S, Levin M, Kaplan DL. Depolarization alters phenotype, maintains plasticity of predifferentiated mesenchymal stem cells. Tissue Eng Part A 2013;19:1889–1908. DOI: 10.1089/ten.tea.2012.0425.rev
54. Sundelacruz S, Levin M, Kaplan DL. Comparison of the depolarization response of human mesenchymal stem cells from different donors. Sci Rep 2015;5:18279. DOI: 10.1038/srep18279
55. Sundelacruz S, Li C, Choi YJ, et al. Bioelectric modulation of wound healing in a 3D in vitro model of tissue-engineered bone. Biomaterials 2013;34:6695–6705. DOI: 10.1016/j.biomaterials.2013.05.040
56. Livak KJ, Schmittgen TD. Analysis of relative gene expression data using real- time quantitative PCR and the 2-ΔΔCT method. Methods 2001;25:402–408. DOI: 10.1006/meth.2001.1262
57. Diaz-Rodriguez P, Chen H, Erndt-Marino JD, et al. Impact of select sophorolipid derivatives on macrophage polarization and viability. ACS Appl Bio Mater 2019;2:601–612. DOI: 10.1021/acsabm.8b00799
58. Tebaykin D, Tripathy SJ, Binnion N, et al. Modeling sources of interlaboratory variability in electrophysiological properties of mammalian neurons. J Neurophysiol 2018; 119:1329–1339. DOI: 10.1152/jn.00604.2017
59. Gerencser AA, Chinopoulos C, Birket MJ, et al. Quantitative measurement of mitochondrial membrane potential in cultured cells: Calcium-induced de- and hyperpolarization of neuronal mitochondria. 2012;12:2845–2871. DOI: 10.1113/jphysiol.2012.228387
60. Palsson-McDermott EM, Curtis AM, Goel G, et al. Pyruvate Kinase M2 regulates Hif-1α activity and IL-1β induction, and is a critical determinant of the Warburg effect in LPS- activated macrophages. Cell Metab 2016;21: 65–80. DOI: 10.1016/j.cmet.2014.12.005.Pyruvate
61. Zhu L, Zhao Q, Yang T, et al. Cellular metabolism and macrophage functional polarization. Int Rev Immunol 2015;34:82–100. DOI: 10.3109/08830185.2014.969421
62. Snider SA, Margison KD, Ghorbani P, et al. Choline transport links macrophage phospholipid metabolism and inflammation. J Biol Chem 2018;293:11600–11611. DOI: 10.1074/jbc.RA118.003180
63. Liu L, Lu Y, Martinez J, et al. Proinflammatory signal suppresses proliferation and shifts macrophage metabolism from Myc-dependent to HIF1α-dependent. Proc Natl Acad Sci U S A 2016;113:1564–1569. DOI: 10.1073/pnas .1518000113
64. Boveris A, Alvarez S, Navarro A. The role of mitochondrial nitric oxide synthase in inflammation and septic shock. Free Radic Biol Med 2002;33:1186–1193. DOI: 10.1016/S0891-5849(02)01009-2
65. Land JM, Hargreaves IP, Brearley D, et al. Mitochondrial dysfunction in sepsis. J Neurol Sci 2002;199(Table 1):DOI: 10.1016/S0140-6736(02)09459-X
66. Baseler WA, Davies LC, Quigley L, et al. Autocrine IL-10 functions as a rheostat for M1 macrophage glycolytic commitment by tuning nitric oxide production. Redox Biol 2016;10:12–23. DOI: 10.1016/j.redox.2016.09.005
67. Van den Bossche J, Baardman J, Otto NA, et al. Mitochondrial dysfunction prevents repolarization of inflammatory macrophages. Cell Rep 2016;17:684–696. DOI: 10.1016/j.celrep.2016.09.008
68. O'Neill LAJ. A metabolic roadblock in inflammatory macrophages. Cell Rep 2016;17:625–626. DOI: 10.1016/j .celrep.2016.09.085
69. Ong ST, Ng AS, Ng XR, et al. Extracellular K + dampens T cell functions: implications for immune suppression in the tumor microenvironment. Bioelectricity 2019;1:169–179. DOI: 10.1089/bioe.2019.0016
70. Natochin YV. The origin of membranes. Paleontol J 2010; 44:860–869. DOI: 10.1134/S0031030110070142

71. Danchin A, Nikel PI. Why nature chose potassium. J Mol Evol 2019. DOI: 10.1007/s00239-019-09915-2
72. Augustynek B, Wrzosek A, Koprowski P, et al. What do we not know about mitochondrial potassium channels? Biochim Biophys Acta Bioenerg 2016;1857:1247–1257. DOI: 10.1016/j.bbabio.2016.03.007
73. Warskulat U, Schliess F, Häussinger D. Compatible organic osmolytes and osmotic modulation of inducible nitric oxide synthetase in RAW 264.7 mouse macrophages. Biol Chem 1998;379:867–874. DOI: 10.1515/bchm.1998.379.7.867
74. Oh KW, Currin RT, Lemasters JJ. Kupffer cells mediate increased anoxic hepatocellular killing from hyperosmolarity by an oxygen- and prostaglandin-independent mechanism. Toxicol Lett 2000;117:95–100. DOI: 10.1016/S0378-4274(00)00247-2
75. Shapiro L, Dinarello CA. Osmotic regulation of cytokine synthesis in vitro. Proc Natl Acad Sci U S A 1995;92:12230–12234. DOI: 10.1073/pnas.92.26.12230
76. Abolhassani M, Wertz X, Pooya M, et al. Hyperosmolarity causes inflammation through the methylation of protein phosphatase 2A. Inflamm Res 2008;57:419–429. DOI: 10.1007/s00011-007-7213-0
77. Sun T, Jackson S, Haycock JW, et al. Culture of skin cells in 3D rather than 2D improves their ability to survive exposure to cytotoxic agents. J Biotechnol 2006;122:372–381. DOI: 10.1016/j.jbiotec.2005.12.021
78. Duval K, Grover H, Han LH, et al. Modeling physiological events in 2D vs. 3D cell culture. Physiology 2017;32:266–277. DOI: 10.1152/physiol.00036.2016
79. Caron MMJ, Emans PJ, Coolsen MME, et al. Redifferentiation of dedifferentiated human articular chondrocytes: Comparison of 2D and 3D cultures. Osteoarthritis Cartilage 2012;20:1170–1178. DOI: 10.1016/j.joca.2012.06.016
80. Breslin S, O'Driscoll L. The relevance of using 3D cell cultures, in addition to 2D monolayer cultures, when evaluating breast cancer drug sensitivity and resistance. Oncotarget 2016;7:45745–45756. DOI: 10.18632/oncotarget.9935
81. Zhang F, Warskulat U, Wettstein M, et al. Hyperosmolarity stimulates prostaglandin synthesis and cyclooxygenase-2 expression in activated rat liver macrophages. Biochem J 1995;312:135–143. DOI: 10.1042/bj3120135
82. Soto-Cerrato V, Manuel-Manresa P, Hernando E, et al. Facilitated anion transport induces hyperpolarization of the cell membrane that triggers differentiation and cell death in cancer stem cells. J Am Chem Soc 2015;137:15892–15898. DOI: 10.1021/jacs.5b09970
83. Chernet BT, Levin M. Transmembrane voltage potential of somatic cells controls oncogene-mediated tumorigenesis at long-range. Oncotarget 2014;5:3287–3306. DOI: 10.18632/oncotarget.1935
84. Chernet BT, Levin M. Transmembrane voltage potential is an essential cellular parameter for the detection and control of tumor development in a Xenopus model. DMM Dis Model Mech 2013;6:595–607. DOI: 10.1242/dmm.010835
85. Lobikin M, Chernet B, Lobo D, et al. Resting potential, oncogene-induced tumorigenesis, and metastasis: The bioelectric basis of cancer in vivo. Phys Biol 2012;9:065002. DOI: 10.1088/1478-3975/9/6/065002
86. Chernet B, Levin M. Endogenous voltage potentials and the microenvironment: bioelectric signals that reveal, induce and normalize cancer. J Clin Exp Oncol 2013; Suppl 1:pii: S1-002. DOI: 10.4172/2324-9110.S1-002
87. Liu B, Poolman B, Boersma AJ. Ionic strength sensing in living cells. ACS Chem Biol 2017;12:2510–2514. DOI: 10.1021/acschembio.7b00348
88. Depaoli MR, Bischof H, Eroglu E, et al. Live cell imaging of signaling and metabolic activities. Pharmacol Ther 2019;202:98–119. DOI: 10.1016/j.pharmthera.2019.06.003
89. Hwang K, Mou Q, Lake RJ, et al. Metal-dependent DNAzymes for the quantitative detection of metal ions in living cells: Recent progress, current challenges, and latest results on FRET ratiometric sensors. Inorg Chem 2019;58:13696–13708. DOI: 10.1021/acs.inorgchem.9b01280
90. Farnsworth NL, Mead BE, Antunez LR, et al. Ionic osmolytes and intracellular calcium regulate tissue production in chondrocytes cultured in a 3D charged hydrogel. Matrix Biol 2014;40:17–26. DOI: 10.1016/j.matbio.2014.08.002
91. Cardin V, Pena-Segura C, Pasantes-Morales H. Activation and inactivation of taurine efflux in hyposmotic and isosmotic swelling in cortical astrocytes: Role of ionic strength and cell volume decrease. J Neurosci Res 1999;56:659–667.
92. Quinn SJ, Kifor O, Trivedi S, et al. Sodium and ionic strength sensing by the calcium receptor. J Biol Chem 1998;273:19579–19586.
93. Kerby GS, Cottin V, Accurso FJ, et al. Impairment of macrophage survival by NaCl: Implications for early pulmonary inflammation in cystic fibrosis. Am J Physiol Lung Cell Mol Physiol 2002;283:188–197.
94. Amin AK, Huntley JS, Patton JT, et al. Hyperosmolarity protects chondrocytes from mechanical injury in human articular cartilage: An experimental report. J Bone Joint Surg B 2011;93 B:277–284. DOI: 10.1302/0301-620X.93B2.24977

Address correspondence to:
Joshua Erndt-Marino, PhD
Department of Biomedical Engineering
Tufts University
Medford, MA 02155

E-mail: josh.marino2@gmail.com

Mariah S. Hahn, PhD
Department of Biomedical Engineering
Rensselaer Polytechnic Institute
Troy, NY 12180-3522

E-mail: hahnm@rpi.edu